

# Quantitative Performance Evaluation of Thinning Algorithms under Noisy conditions

M. Y. Jaisimha, Robert M. Haralick and Dov Dori\*  
Dept. of Electrical Engineering,  
University of Washington  
Seattle, WA 98195

\*Faculty of Industrial Engineering and Management,  
Technion, Israel Institute of Technology  
Haifa 32000, Israel

## Abstract

Thinning algorithms are an important sub-component in the construction of computer vision (especially for Optical Character Recognition (OCR)) systems. Important criteria for the choice of a thinning algorithm include the sensitivity of the algorithms to input shape complexity and to the amount of noise. In previous work, we introduced a methodology to quantitatively analyze the performance of thinning algorithms. The methodology uses an ideal world model for thinning based on the concept of Blum ribbons. In this paper we extend upon this methodology to answer these and other experimental questions of interest. We contaminate the noise-free images using a noise model that simulates the degradation introduced by the process of Xerographic copying and laser printing. We then design experiments that study how each of 16 popular thinning algorithms performs relative to the Blum ribbon gold standard and relative to itself as the amount of noise varies. We design statistical data analysis procedures for various performance comparisons. We present the results obtained from these comparisons and a discussion of their implications in this paper.

**Keywords:** Performance Evaluation, Thinning Algorithms.

## 1 Introduction

This paper presents a quantitative methodology for characterizing the performance of thinning algorithms. A large number of papers proposing thinning algorithms have been published in the literature. A comprehensive survey is given in [5]. A key issue in the performance evaluation of thinning algorithms is the choice of the "gold standard" or reference with respect to which the output of the algorithm is compared. Previous efforts to provide a quantitative performance measure have used a subjective "gold standard" provided by a "panel of experts." [6],[8]. One obvious limitation of this approach is the infeasibility of conducting an exhaustive study/analysis of the perfor-

mance over a wide range of operating conditions since the gold standard for each instance must be specified interactively by the expert. This is too expensive to do for large numbers of input images, leading to small sample sizes, which, in turn prevent us from being able to draw statistically significant conclusions from the data.

In this investigation we propose to overcome the limitations of the expert approach in two ways. We first define an objective gold standard based on Blum ribbons, where the expected output of the ideal thinning algorithm is the spine of the ribbon. We present results that indicate that our experimental conclusions are the same whether we use the Blum ribbon or the output of the thinning algorithm under noise-free conditions as a gold standard.

Since thinning forms an important component in many OCR systems, it is important to accurately estimate the performance of thinning algorithms. Also, all real-world document imagery is contaminated to a greater or lesser extent by random perturbations or noise. It is important to choose a thinning algorithm that is relatively insensitive to noise or whose performance degrades relatively gracefully as the amount of noise in the input image increases and as the geometry of the input shapes change. This investigation will enable us to make these choices in a precise and quantitative manner.

We discuss briefly issues pertinent to the performance characterization of thinning algorithms in Section 2. We present the ideal world model for thinning based on Blum ribbons in Section 2.1. Once an ideal world model for thinning has been introduced, the next task is to choose a perturbation model that adequately models the degradations found in document images. We use the degradation model proposed by Kanungo et. al. [4] that models the degradation of documents due to photocopying and printing. Since, printed/photocopied document images form a large fraction of the images input to a typical OCR system, we use this perturbation model in our investigation to introduce controlled perturbations in our input images and then study the performance of the thinning

algorithms under noisy conditions. We briefly review the degradation model in Section 4. For the error criterion function that measures the deviation between the output of the thinning algorithm and the ideal expected results, we use an error criterion function based on the Hausdorff distance Section 3. The performance characterization experiments and the results obtained are described in Section 6. We present our conclusions in Section 7.

## 2 Performance Characterization of Thinning

The most popular application for thinning algorithms is in the field of Optical Character Recognition (OCR). Thus, it is important that the shapes under consideration should model the shapes that OCR algorithms operate on - namely characters (printed or handwritten). It should be possible to analytically compute the skeleton of the input shape under noise-free conditions and the "skeleton" of the shape should fit commonly held notions of what a skeleton of a shape should be. Given all these criteria we choose ribbons (specifically Blum Ribbons) as our ideal world model for the world of thinning algorithms.

Blum ribbons are generated by sweeping a generating disk (whose radius might vary) along a two dimensional curve. The gold standard for our performance evaluation is given by the spine of the Blum ribbon. The error criterion function is based on the Hausdorff error metric. We expect to find differences in performance to show up even when the ribbon images are noise-free. In addition when noise is added to the input images, we expect different thinning algorithms to respond differently as the amount of noise varies.

### 2.1 Blum Ribbons as an Ideal World Model

A ribbon is defined as the shape obtained when a shape referred to as the "generator" is swept along a curve. The ideal world of shapes to be thinned is the world of Blum ribbons. Blum ribbons are constructed when the generator is a disk.

At any point of the the arc, the width of the ribbon is the length of the line segment defined by the intersection of the ribbon with a line perpendicular to the arc at the given arc point. The cross-section function has bounded first derivatives to keep the width from changing too fast. The width itself is also bounded from both sides, to prevent too narrow or too wide ribbons. Additionally, there is a relation between the maximum allowed curvature (minimum local radius) of the arc and the maximum allowed width of the ribbon, in order to prevent a case in which the combination of sharp curvature and large width at that point cause the ribbon to overlap itself. An ideal digital image is constructed from a scene of ribbons by tessellating the scene of ribbons into pixels.

The Blum ribbon is illustrated in Figure 1.

To avoid problems of instability when the slope of the spine approaches 90°, and to enable self intersec-

tion of the spine, we adopt the following parametric description for the spine  $S$ .

$$S(s) = \begin{pmatrix} x(s) \\ y(s) \end{pmatrix}$$

The scalar function that describes the radius of the generating disc sweeping along  $S$  is called the *contour function* and denoted by  $C(s)$ .

In order for the ribbon to be useful in characterizing the performance of a thinning algorithm, the radius of the generator has to be small relative to the radius of curvature of the spine in order to prevent the ribbon from intersecting itself in order for the ribbon to be useful in the performance evaluation of thinning algorithms. If the maximum value of the radius function is less than the minimum value of the radius of curvature of the spine, this sort of situation can be avoided. Specifically, if

$$\rho_{max} < \frac{(\dot{x}^2 + \dot{y}^2)^{2/3}}{|\ddot{x}\dot{y} - \dot{x}\ddot{y}|}$$

where  $\rho_{max}$  is the maximum value of the radius function and the terms  $\dot{x}$ ,  $\dot{y}$ , and  $\ddot{x}$ ,  $\ddot{y}$  are the first and second order derivatives of the  $x$  and  $y$  components of the spine. These components are expressed in parametric form parameterized by the arc length  $s$ . Then,  $\rho_{min}$  is the minimum value of the radius of curvature of the spine. Once we assume a form for the functions  $x(s)$ ,  $y(s)$  and  $C(s)$  (the contour function, which, in our case, is the radius function), the problem of generating a ribbon becomes one of choosing the parameters of the form such that the constraints mentioned above are satisfied. For the purposes of this study we assume that the spine polynomial components are of the form  $x(s) = \sum_{i=0}^{i=3} a_i s^i$  and  $y(s) = \sum_{i=0}^{i=3} b_i s^i$

Thus, the highest power of  $s$  in either the  $x$  or  $y$  component is 3. Further, we assume that the radius function takes the form

$$C(s) = \sum_{i=0}^{i=2} c_i s^i$$

Generating a ribbon thus reduces to the problem of choosing the coefficients  $a_i$ ,  $b_i$  and  $c_i$  to satisfy the constraints on the curvature of the spine relative to the value of the radius function. Two images are generated. One contains the discretized version of the spine and the other contains a discretized version of the ribbon.

## 3 Error Criterion Function

Thinning can have a variety of purposes such as the estimation of the analytic expression for the spine of the ribbon or the identification of the pixels through which the spine passes. In this discussion we take the purpose of thinning to be the identification of the pixels through which the spine passes. We use as the error criterion, a metric based on the Hausdorff distance [1]. We measure the Hausdorff distance between the gold standard and the output of the thinning algorithm. Given two sets  $A$  and  $B$  and a distance metric  $\rho$ , the Hausdorff distance is given by

$$\max(\rho(A, B), \rho(B, A)) =$$

$$\max\{\inf\{r|A \subseteq B \oplus \text{disk}(r)\}, \inf\{r|B \subseteq A \oplus \text{disk}(r)\}\}$$

The Hausdorff distance provides a measure of the farthest distance between two sets. The Hausdorff distance can also be alternately interpreted as the maximum of the shortest distances between every point on one curve and the second curve. We use a method based on the Euclidean distance transform of the two images - the Blum spine and the output of the thinning algorithm to compute the Hausdorff distance.

Computationally, the maximum value of the error criterion function is half the larger of the row or column size of the image. In order to make the error criterion invariant with the size of the image, we use a normalized error criterion given by

$$\epsilon_1 = \varrho(S, T) / (N_{ROWS} / 2)$$

where  $\epsilon_1$  is the normalized error criterion function,  $S$  is the spine of the Blum ribbon,  $T$  is the output of the thinning algorithm and as before  $\varrho(S, T)$  denotes the Hausdorff distance between the two.

## 4 Noise Model

In this section we briefly review the noise model proposed in [4] that we use as a degradation model in our study. Degradations in bi-level document images consist of foreground pixels becoming background pixels and vice-versa. Briefly, the degradation model operates as follows:

- The probability of a pixel in the foreground  $I_F$  of the image at  $(r, c)$  (denoted by  $I_F(r, c)$ ) becoming a background pixel is given by  $c_0 + \alpha_0 e^{-\alpha d_F^2(r, c)}$  where  $d_F(r, c)$  is the Euclidean distance to the nearest background pixel.
- The probability of a pixel in the background  $I_B$  at  $(r, c)$  (denoted by  $I_B(r, c)$ ) becoming a foreground pixel is given by  $c_0 + \beta_0 e^{-\beta d_B^2(r, c)}$
- Correlation is then introduced in the degraded image by performing a binary morphological closing with a digital disk of diameter  $K$ .

The model is parameterized by  $\alpha, \alpha_0, \beta, \beta_0$  and  $c_0$ . For the purposes of the experiment we hold the following values fixed:  $c_0 = 0$ , and  $\alpha_0$  and  $\beta_0$  take values from the set  $\{0, 1\}$ . The parameter  $\alpha$  influence the amount of "thinning" of the foreground in the image that takes place while  $\beta$  influences the "thickening" of the foreground.

## 5 Computational Procedure for Generating Ribbon Images

Once we assume a form for the functions  $x(s), y(s)$  and  $C(s)$  (the radius function) the problem of generating a ribbon becomes one of choosing the coefficients  $a_i, b_i$  and  $c_i$  so constraints mentioned previously (Section 2.1) are satisfied.

The user supplies as input to the procedure the following inputs: Maximum degree of the spine polynomials for the  $x$  and  $y$  components, Maximum degree of the radius polynomial, Number of rows and columns in the image and the aspect value (this is the ratio of the length of the spine to the maximum value that the radius function can take).

The procedure for picking coefficients is as follows

1. Generate coefficients between -1.0 and +1.0 for each of the polynomial components of the spine. For the coefficient  $a_i$  of the  $x$  component we have  $a_i \sim U(-1, 1)$  where  $U(-1, 1)$  is a uniformly distributed random variable on the interval  $[-1, 1]$ . The coefficients  $b_i$  for the  $y$  component are also given by  $b_i \sim U(-1, 1)$
2. Compute the minimum radius of curvature for the spine polynomial specified by the coefficients  $a_i$  and  $b_i$ .
3. Generate coefficients  $c_i$  for the radius function using  $c_0 \sim U(0.1, 1)$  and  $c_i \sim U(0.0, 1.0)$  for  $i > 0$  where  $U(0, 1)$  is a uniformly distributed random variable in the interval  $(0, 1)$ . The coefficients are then scaled to satisfy the Blum ribbon generation condition given by  $|C'(s)| < 1$  and so that the maximum value of the radius function does not exceed the minimum radius of curvature.

## 6 Experiments for Performance Characterization

### 6.1 Population of Input Images

We define various populations of images based on the parameters used as input to the image generation process. We vary only the degree of  $x$  and  $y$  components of the spine polynomial and the degree of the radius function polynomial. We hold the image size fixed at  $128 \times 128$  and the aspect value fixed at 5.0. Letting  $d_x$  be the degree of the  $x$  component of the spine polynomial,  $d_y$  be the degree of the  $y$  component of the spine polynomial and  $d_r$  be the degree of the radius function we define six image populations by taking  $d_x = 1, d_y = 0, 1$  or  $2$  and  $d_r = 0, 1$  or  $2$ . In Figure 2 we show an example Blum ribbon image with the spine overlaid on the ribbon.

### 6.2 Thinning Algorithms under Investigation

We evaluate sixteen thinning algorithms in this study. They are based on distance transform methods (Algorithm 1) (Arcelli), binary picture thinning by an iterative parallel two-subcycle operation (Algorithm 2), (Suzuki and Abe, Pattern Recognition 1987) two different distance transform based algorithms (Algorithm 3 and 4) (Suzuki and Abe ICPR 1986), morphological thinning algorithm (does not give connected skeletons) (Algorithm 5), Arcelli's Parallel Thinning algorithm (Algorithm 6), Parallel thinning (Algorithm

Table 1: P values for 1-way ANOVA with  $d_r$  as a factor

	P		P
Alg. 1	1.26104e-10	Alg. 9	6.176975e-06
Alg. 2	0.2431301	Alg. 10	7.370414e-08
Alg. 3	0.05136805	Alg. 11	0.04476234
Alg. 4	8.55982e-14	Alg. 12	0.002871999
Alg. 5	8.55982e-14	Alg. 13	0.02609825
Alg. 6	9.143812e-07	Alg. 14	4.218959e-12
Alg. 7	9.358232e-06	Alg. 15	2.994326e-07
Alg. 8	1.073249e-09	Alg. 16	0.00863055

7), Rutovitz Algorithm (Algorithm 8), E.S. Deutsch's Algorithm (Algorithm 9), Tamura's Algorithm (Algorithm 10), Ma and Yudin Algorithm (Algorithm 11), SPTA thinning (Algorithms 12 and 14), Stefanelli and Rosenfeld (Algorithm 13), Hilditch's algorithm (Algorithm 15) and Zhang's algorithm. (Further references for the algorithms can be found in [3].)

### 6.3 Performance Characterization under Noise-Free conditions

As we had mentioned in the Introduction, we expected differences in algorithm performance to show up even under noise-free conditions. In this experiment we generate 250 images of each of the six combinations of the values of  $d_y$  (the degree of the  $y$  component of the spine polynomial) and  $d_r$  (the degree of the radius function). Each of these images is then input to the sixteen thinning algorithms under investigation. We compute the error criterion function relative to the Blum ribbon gold standard for each of the algorithm outputs.

#### 6.3.1 Data Analysis and Results

We use a One-way Fixed effects ANOVA model ([7]) to analyze the effect the various factors ( $d_x$ ,  $d_y$  and  $d_r$ ) have on the performance of the various thinning algorithms as quantified by the normalized Hausdorff distance. The null hypothesis for the first test is that the mean of the error criterion function is invariant with respect to the degree of the radius function  $d_r$  when all other parameters are held fixed for each of the thinning algorithms.

The following table (Table 1) lists the P values obtained for each the 16 algorithms for  $d_y = 2$  and  $d_r$  takes values from the set  $\{0, 1, 2\}$ . The P value is the probability of the null hypothesis being true given the data. If the probability P is greater than a pre-specified significance level, we accept the null hypothesis.

We can see that the null hypothesis (that the algorithms perform equally well at all three levels of  $d_r$ ) can be rejected at a significance level of 0.05 for all but Algorithms 2 and 3. At a significance level of 0.005 we can accept the null hypothesis for Algorithms 11, 13 and 16 too.

Table 2: P values for two way ANOVA with  $d_y$  and  $d_r$  as factors

	$P_y$	$P_r$	$P_{yr}$
Alg. 1	0.000000	0.000000	0.000115
Alg. 2	0.000000	0.203913	0.307711
Alg. 3	0.002184	0.000003	0.056927
Alg. 4	0.1221822	0.0000086	0.3334617
Alg. 5	0.00017562	0.000000	0.02939563
Alg. 6	0.0125985	0.00000	0.2762129
Alg. 7	0.0310419	0.0000001	0.1317269
Alg. 8	0.9898693	0.0000000	0.1570388
Alg. 9	0.000000	0.000000	0.1051961
Alg. 10	0.1520182	0.00000	0.2857383
Alg. 11	0.000000	0.0018602	0.4866845
Alg. 12	0.000000	0.000000	0.1317364
Alg. 13	0.000000	0.0001285	0.3613095
Alg. 14	0.00146164	0.000000	0.05356874
Alg. 15	0.1118477	0.000000	0.1422055
Alg. 16	0.0026202	0.0026202	0.2476276

Similarly we can now pose a null hypothesis relative to the value of  $d_y$  when  $d_r$  is held fixed. Alternatively, we can use a two-way fixed effects ANOVA model and explore interactions between the two factors  $d_y$  and  $d_r$  which are a measure of the complexity of the input shapes. We present the P values for each of the three factors ( $d_y$  and  $d_r$  and interactions) for each of the 16 algorithms in Table 2. The column  $P_y$  contains the P values obtained for the factor  $d_y$ ,  $P_r$  are the P values obtained for factor  $d_r$  and  $P_{yr}$  are the P values obtained for the interaction of the two factors.

At a significance level of 5% we can reject the null hypothesis for the factor  $d_y$  for all but Algorithms 4, 5 and 15. Algorithm 8 is clearly insensitive to the factor  $d_y$  but is highly sensitive to the factor  $d_r$ . The only algorithms to show any significant interactions are Algorithms 1 and 5 (here the P value is lower than the significance level causing the null hypothesis to be rejected). An ideal algorithm (in terms of being invariant to the geometry or complexity of the input shape) would have high P values for both factors and their interaction. Algorithm 1 is highly sensitive to the geometry of the input shape since the P value is lower than the significance level for all three factors.

### 6.4 Performance Characterization under Noisy Conditions

In this experiment, we study the effects of noise on the performance of thinning algorithms. We conduct two sub-experiments to study how each of these two kinds of degradation influence the performance of the thinning algorithms.

For each of these experiments we generate 250 ribbon and spine images for each of the six combinations of the values of  $d_y$  and  $d_r$ . The noise-free images are first input to the sixteen thinning algorithms to produce thinning algorithm outputs. Noise is then added to the ribbon image and the noisy image is then input to the thinning algorithms. We then measure the

Table 3: P values for one way ANOVA with  $\beta$  as a factor and Error criterion computed relative to the Blum spine

	P		P
Alg. 1	0.3793848	Alg. 9	7.576662e-11
Alg. 2	0.003407573	Alg. 10	2.079902e-07
Alg. 3	0.04085983	Alg. 11	0.0008889729
Alg. 4	0.008688507	Alg. 12	0.0310366
Alg. 5	0.1717833	Alg. 13	0.0007498882
Alg. 6	1.945989e-08	Alg. 14	0.1761424
Alg. 7	5.177823e-06	Alg. 15	0.1821755
Alg. 8	0.0192007	Alg. 16	3.099773e-10

Hausdorff distance between the output of the thinning algorithm under noisy conditions and the Blum spine of the ribbon or the output of the thinning algorithm under noise-free conditions. In Figure 3 we show the ribbon of Figure 2 with noise added using the degradation model. Figure 4 shows the noise-free ribbon overlaid with the output of Algorithm 1 when the noise-free ribbon is used as input. Figure 5 shows the noisy ribbon overlaid with the output of Algorithm 1 when the noisy ribbon is used as input. The three Hausdorff distances we can measure are between the noise-free output and the Blum spine, the noisy output and the Blum spine, and, the noisy output and the noise-free output.

#### 6.4.1 Data Analysis and Results

In the first illustration we wish to answer two questions: 1) How do each of the algorithms perform in the presence of varying levels of "thickening" degradation? 2) How does the choice of reference skeleton (Blum spine vs. noise-free algorithm output) influence the conclusions on algorithm performance?

We use the one-way ANOVA model to analyze the results obtained. Table 3 shows the P values for each of the 16 algorithms for  $d_y = 2$  and  $d_r = 2$  when the null hypothesis is that the mean values of the error criterion (Hausdorff distance measured with respect to the Blum spine) are equal for all four noise levels  $\beta \in \{0.1, 0.2, 0.3, 0.4\}$ . We can see that at a 5% significance level, we can accept the null hypothesis (that the algorithm performance does not greatly vary with noise level) for Algorithms 1, 5, 14 and 15. These algorithms exhibit performance that is relatively insensitive with respect to noise. The smaller the P value for an algorithm, the more variable the quality of the algorithm output is with respect to noise. Algorithm 9 and 16 are relatively sensitive with respect to the noise level for this image population.

Table 4 shows the P values for the same experiment when the error criterion is the Hausdorff distance is computed with reference to the noise-free output of the thinning algorithm. Clearly, the P values computed using this reference skeleton are different from those of Table 4. However, we find that at a 5% significance level we can accept the null hypothesis (of equal performance) for Algorithms 1, 5, 14 and 15 (as

Table 4: P values for one way ANOVA with  $\beta$  as a factor and Error criterion computed relative to the noise-free thinning algorithm output

	P		P
Alg. 1	0.1891778	Alg. 9	1.046807e-11
Alg. 2	3.369093e-09	Alg. 10	1.242838e-08
Alg. 3	3.420988e-06	Alg. 11	5.417444e-11
Alg. 4	0.01328209	Alg. 12	2.967738e-07
Alg. 5	0.1493699	Alg. 13	8.881784e-16
Alg. 6	1.760964e-09	Alg. 14	0.09892299
Alg. 7	5.889878e-06	Alg. 15	0.1007167
Alg. 8	0.02841082	Alg. 16	6.478187e-11

Table 5: P values for 1 way ANOVA with both "thickening" and "thinning" noise

	P		P
Alg. 1	0.6720077	Alg. 9	0.00000
Alg. 2	3.704943e-08	Alg. 10	0.00000
Alg. 3	3.876884e-06	Alg. 11	7.796093e-09
Alg. 4	0.01328209	Alg. 12	0.01481161
Alg. 5	0.8422798	Alg. 13	3.29613e-08
Alg. 6	0.000000	Alg. 14	0.8830483
Alg. 7	1.171288e-13	Alg. 15	0.7882021
Alg. 8	0.03366714	Alg. 16	0.000000

in the previous case). Once again, Algorithms 9 and 16 are the most sensitive to noise. Thus the inferences we can make from the data do not change based on what we use as the gold standard! We have strong evidence to conclude that the Blum spine is a suitable gold standard for performance evaluation of thinning algorithms. Also, while the Blum spine may vary from what many algorithm developers may refer to as the ideal skeleton, the diagnostic efficiency (so to speak) of the Blum spine is high.

In the second sub-experiment we study the performance of the thinning algorithms when both varieties of degradation are present. The noise parameters we use are  $\alpha_0 = 1$ ,  $\beta_0 = 1$ ,  $c_0 = 0.0$ . The four noise levels we study have the following parameters -  $\{\alpha = 0.1, \beta = 0.1\}$ ,  $\{\alpha = 0.2, \beta = 0.2\}$ ,  $\{\alpha = 0.3, \beta = 0.3\}$  and  $\{\alpha = 0.4, \beta = 0.4\}$ . We use a one-way ANOVA model to study the performance of the thinning algorithms for a particular image population  $d_y = 2$  and  $d_r = 1$ . The null hypothesis under consideration is that the mean value of the error criterion function remains the same for different values of the noise level. The P values measured relative to the Blum ribbon are shown in Table 5. The null hypothesis can be accepted at a significance level of 5% for Algorithms 1, 5, 14 and 15. These results are identical to the conclusions drawn from Tables 4 and 5.

## 7 Conclusions and Work in Progress

We have presented a methodology for the performance evaluation of thinning algorithms. We describe

mechanisms to generate ideal world images based on the Blum ribbon model. We then used a degradation model that simulates perturbations found in real-life document images to introduce noise in the ideal world images. We designed experiments to study the performance of 16 thinning algorithms under different perturbations and image populations. We then use measurements of the Hausdorff error criterion function in conjunction with powerful statistical ANOVA tests to compare the performance of thinning algorithms. We are able to identify candidate algorithms whose performance is relatively insensitive to noise level and complexity of the input shape. We also show that the Blum ribbon permits us to make valid inferences about algorithm performance.

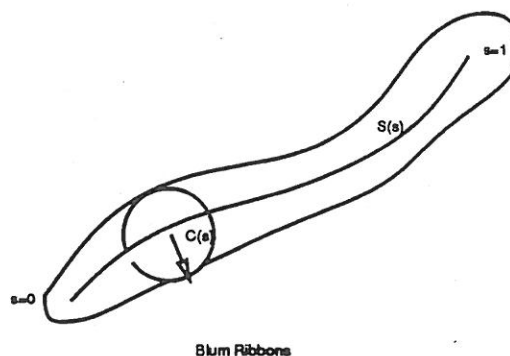


Figure 1: Blum Ribbons

## References

- [1] Haralick, R. M., and Shapiro, L. G., *Computer and Robot Vision*, Addison-Wesley Inc. 1992.
- [2] Jaisimha, M. Y., Haralick, R. M., and Dori, Dov M., "A Methodology for the Quantitative Performance Characterization of Thinning Algorithms," *Proc. Second International Conference on Document Analysis and Recognition*, October 1993, Tsukuba City, Japan.
- [3] Jaisimha, M. Y. and Haralick, R. M., "Quantitative Performance Characterization of Thinning Algorithms in the presence of noise," Intelligent Systems Laboratory Technical Report, March 1994.
- [4] Kanungo, T., Haralick, R. M., and Phillips, I. T., "Global and Local document degradation models," *Proc. Second International Conference on Document Analysis and Recognition*, October 1993, Tsukuba City, Japan.
- [5] Lam, L., S.-W. Lee, and C. Y. Suen, "Thinning Methodologies, a Comprehensive Study," *IEEE Transactions on Pattern Analysis and Machine Intelligence*, Vol. 14 No. 9, 1992, pp. 869-85.
- [6] Lee, L. Lam and C. Y. Suen, "Performance Evaluation of Skeletonization Algorithms for Document Image Processing," *Proc. IAPR First Int'l Conf. on Document Analysis and Recognition*, Saint Malo, France, October 1991, Vol. 1, pp. 260-71.
- [7] Lindman, Harold R., *Analysis of Variance in Experimental Design*, Springer-Verlag., 1992
- [8] Plamondon, R., Bourdeau, M., Chouinard, C., and Suen, C. Y., "Validation of Preprocessing Algorithms: A Methodology and its Application to the Design of a Thinning Algorithm for Handwritten Characters," *Proc. Second International Conference on Document Analysis and Recognition*, October 1993, Tsukuba City, Japan.

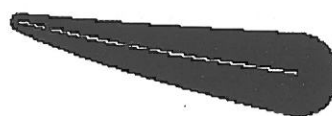


Figure 2: Ribbon with  $d_r = 2$ ,  $d_l = 2$



Figure 3: Ribbon with noise



Figure 4: Output of Algorithm 1 for noise-free ribbon



Figure 5: Output of Algorithm 1 for noisy ribbon